

Original Research

Enhanced Efficiency of Polycrystalline Silicon Solar Cells Using Electrospayed ZnO-Si₃N₄ Hybrid Antireflective Coatings

R. Meenakshi Reddy ¹, Anu Tonk ², Vishal Shukla ³, P. Vignesh ⁴, S. Karthikeyan ^{5,*}, Chetty Manna Sheela Rani ⁶, Raj Kumar Gupta ⁷, Ramesh Kumar ⁸, T. Thirugnanasambandhami ⁹

¹ Department of Mechanical Engineering, G. Pulla Reddy Engineering College, Kurnool, Andhra Pradesh, India;

² Department of Multidisciplinary Engineering, The NorthCap University, Gurugram, India;

³ Department of Mechanical Engineering, Ramdeobaba University, Nagpur 440013, India;

⁴ Department of Safety and Fire Engineering, K.S.R. College of Engineering, Tiruchengode, Tamil Nadu, India;

⁵ Department of Mechanical Engineering, Erode Sengunthar Engineering College, Perundurai 638057, India;

⁶ Department of Computer Science Engineering, Koneru Lakshmaiah Education Foundation, Guntur 522302, India;

⁷ Department of Physics, Sardar Vallabhbhai Patel College, Bhabhua, Kaimur, Bihar 821101, India;

⁸ Department of Mechanical Engineering, Adithya Institute of Technology, Coimbatore 641107, India;

⁹ Department of Mechanical Engineering, Saveetha School of Engineering, Saveetha Institute of Medical and Technical Sciences (SIMATS), Saveetha University, Chennai 602105, Tamil Nadu, India.

* Correspondence: karthiksamynathan@gmail.com

Received: December 4, 2025; Accepted: April 10, 2026

Abstract: For the current global energy demand, the solar based energy resource was found to be long term, consistent and renewable in nature. Present research work mainly focusses on improving the energy conversion rate of polycrystalline silicon solar cell through antireflective thin films. Polycrystalline silicon solar cell is found to be one of the predominant energy resources for the easier conversion and utilisation of incident light energy into electrical energy. The materials such as zinc oxide (ZnO) and silicon nitride (Si₃N₄) were found to be the excellent antireflection property which hinders the light reflectance. The solar cell was coated with ZnO, Si₃N₄ and ZnO- Si₃N₄ through electrospaying technique. The coated solar cell films were inspected through optical, electrical, structural, elemental and morphological studies. ZnO- Si₃N₄ coated solar cell exert a maximum power conversion efficiency (PCE) of 21.78 % in the controlled light source environment. However, the mechanical blends were found to have higher impact in trapping incident light over the coated surface than the individual material coatings.

Keywords: solar energy; zinc oxide; silicon nitride; electrospaying; light harvesting; anti-reflection coatings; silicon solar cells.

1. Introduction

The fossil fuel energy resource found to be predominant and were satisfying the current energy demand. Even though the conventional energy resource was promising one, it leaves certain toxic greenhouse gases which was affecting current global environment. With the help of solar heat collectors and photovoltaic cells, Solar energy can be effectively utilised as thermal

energy and electrical energy [1, 2]. The performance of solar cells was been enhanced by surface texturing, antireflection thin film coatings, management of light in back and rear surfaces. Also, with the alteration of various layers in the cell architecture of solar cell might also improve the overall performance. Around 30 % of incident light get reflected back from the solar cell surface [3]. This can be reduced through antireflection thin surface films which further improves the overall performance of solar cell. These coating provide the destructive interference between various light waves incident over the solar cell surface. As the thickness of AR coating is engineered to be around one-quarter of the incident light wavelength, destructive interference takes place and thus reflection losses decrease. The chosen antireflection coating material should have refractive indices between the air and solar surface material (probably silicon). In addition to this, it should be the transparent material [4].

Some of the commonly used techniques for the coating of antireflection materials were atomic layer deposition, low-pressure chemical vapour deposition (CVD), plasma enhanced CVD, spin coating, spray coating, screen printing, knife edge coating, brush painting, sputter deposition etc., Moreover, the antireflection materials used for the reduction of reflection loss in solar cells were TiO_2 , Si_3N_4 , MoS_2 , MoSe_2 , ZnO , Ta_2O_5 , SiO_2 , Al_2O_3 etc.,[5-7]. Antireflection coating with better hydrophobicity, Hardness, abrasion resistance etc., will show a better option for reducing the incident light reflection. Antireflection coatings were found to be homogenous, uniformly distributes, optically transparent and appropriate adhesion over coated surface. For the proper reduction of reflection loss, the selected antireflection material coated over solar cell surface should hold the refractive index between the refractive index of air medium and silicon (in case of polycrystalline silicon solar cell). The selected antireflection materials are ZnO , Si_3N_4 and $\text{ZnO-Si}_3\text{N}_4$ mechanical blends which holds the refractive indices as 1.9, 2.4 and 2.2 respectively. ZnO is generally used as antireflection material, buffer layer in second and third generation solar cells, transparent conducting oxide, protective coatings with combined antireflection and transparent conduction oxide property and LED encapsulation material [8]. Similarly, silicon nitride is also utilised as antireflection coating, wear resistant coatings over tools and dies, corrosion resistant coatings in chemical processing equipment, thermal barrier coatings in high temperature environments, orthopaedic implants, biosensors, better surface passivation layer for reducing recombination, optical and beam filters [9]. The preferred coating technique for obtaining antireflection surface was electro spraying. It is a process of disseminating the dispersed coating material maintained at opposite potential of 17 kV with the depositing plate due to the strong electrostatic force of attraction. There is a generation of Taylor cone under optimal mass flow rate, plate speed and input voltage leading to splitting of fine droplets of dispersed liquid [10]. However, the dispersed coating liquid was ejected based on preset mass flow rate. The coating film was found to be uniform after the coating time of 1 hour.

The present work aims to electro spray antireflective thin films of ZnO , Si_3N_4 , $\text{ZnO-Si}_3\text{N}_4$ blends over polycrystalline silicon solar cell. The coated solar cell was inspected under neodymium light source for examining its generated current-voltage output. The control over the coating thickness was a major concern, however from various trials and literature studies the optimal operating parameters of electro spraying was evaluated. With the aid of various characterisation techniques such as Field Emission Scanning Electron Microscope (FESEM), Atomic Force Microscope (AFM), Current-Voltage (I-V) characteristics, electrical resistivity and X-ray Diffraction (XRD), the best performing solar cell was identified under optimal operating conditions. Availability of selected coating material was found to be abundant and available at low cost leads to the cost effective antireflection thin film fabrication over the solar cell surface. This also leads to the further scalability of obtained antireflection layer over polycrystalline silicon solar cell. Figure 1 outlines the detailed preparation process for the synthesis of ZnO , Si_3N_4 and $\text{ZnO-Si}_3\text{N}_4$ AR coatings on polycrystalline silicon solar cells. The procedure involves powder

blending, suspension formulation in ethanol, electro spraying deposition under optimized conditions succeeded by thermal processing in order to achieve coating adhesion and stability over the cell surface. This research presents a ZnO-Si₃N₄ hybrid AR coating applied by an electro spraying process, providing a simple and economical alternative to traditional deposition methods. The hybrid coating enhances refractive index alignment and light entrapment, thereby diminishing surface reflectance. The coated solar cell attained a superior power conversion efficiency of 21.78% relative to the bare cell.

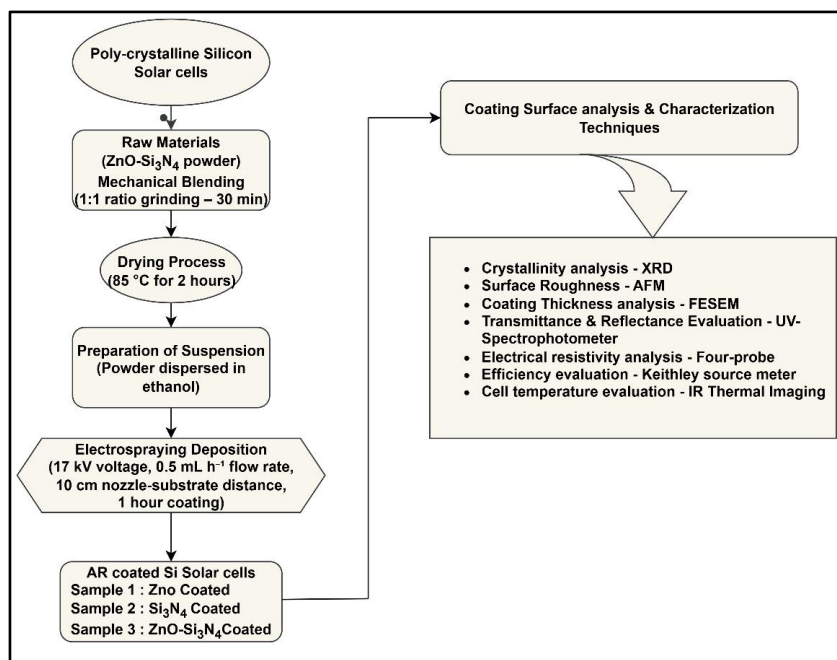


Figure 1. Flowchart of ZnO, Si₃N₄ and ZnO-Si₃N₄ antireflection coating on solar cell substrates.

2. Experimental part

2.1. Materials and chemicals

ZnO, Si₃N₄ were procured with 99% purity from Merck Private Ltd (India). Ethanol with 99.9% purity was purchased from Herenba Instruments and Engineers (India). Polycrystalline silicon solar cells with 0.038 m x 0.052 m dimensions were purchased from Ecoworthy (China).

2.2. Preparation of ZnO- Si₃N₄ mechanical blends

To fabricate the mechanical blends, equal proportion of ZnO and Si₃N₄ powders were taken into mortar and pestle arrangement. It is the traditional and low-cost method where the pestle was firmly pressed against the mortar for certain period of time for the mixing of powder materials in laboratory scale. The powdered particles under repeated crushing leads to deagglomeration, intermixing and internal fracture leading to fine intermixing of powder particles. Using proper weighing balance, ZnO and Si₃N₄ were taken in equal quantity. Before mixing, mortar was cleaned properly and maintained at vacuum to avoid contamination and inclusion of dust particles. ZnO and Si₃N₄ powders, with typical particle dimensions of 20-40 nm and 25-50 nm were employed as AR coating materials. The powders were combined in an identical weight ratio (1:1) to create the ZnO-Si₃N₄ mechanical blend. ZnO and Si₃N₄ powders were combined in an equal weight ratio utilizing a mortar and pestle. The powders were continuously mixed for 30 minutes to achieve consistent blending and deagglomeration of particles. Ethanol was included during grinding at a powder-to-solvent ratio of 1:5 (w/v) to ensure homogeneous particle dispersion. This mixture then

underwent drying in a hot air oven at 85°C for 2 hours to eliminate residual solvent. The dry powder was further finely milled to achieve a homogeneous ZnO-Si₃N₄ mechanical blend before electrospaying.

2.3. Coating of ZnO, Si₃N₄ and ZnO- Si₃N₄ mechanical blends

The electrospaying procedure involved to disperse ZnO, Si₃N₄, and ZnO-Si₃N₄ powders in ethanol to form a precursor solution with a solid concentration of 5 wt%. The suspension was magnetically agitated for 15-20 minutes to achieve homogeneous particle distribution. The prepared suspension was introduced into a 5 mL syringe linked to the electrospaying apparatus. The coating was applied at a voltage of 17 kV, with a solution flow rate of 0.5 mL/h and a nozzle-to-substrate distance of 10 cm. The coating procedure was sustained for one hour, facilitating consistent thin layer development on the surface of the solar cell. Following deposition, the coated samples underwent heat treatment at 100 °C for 30 minutes to improve film adherence and stability.

3. Results and discussion

In order to determine the crystal size, strain in materials, crystal structure and phase composition for a powder material, X-ray diffraction was preferred. With the help of Cu K radiation, the samples to be examined through Rigaku D/Mmax 2500 PC diffractometer. The incident X-ray gets incident over the inspected crystalline sample resulting in the formation of constructive interference [11].

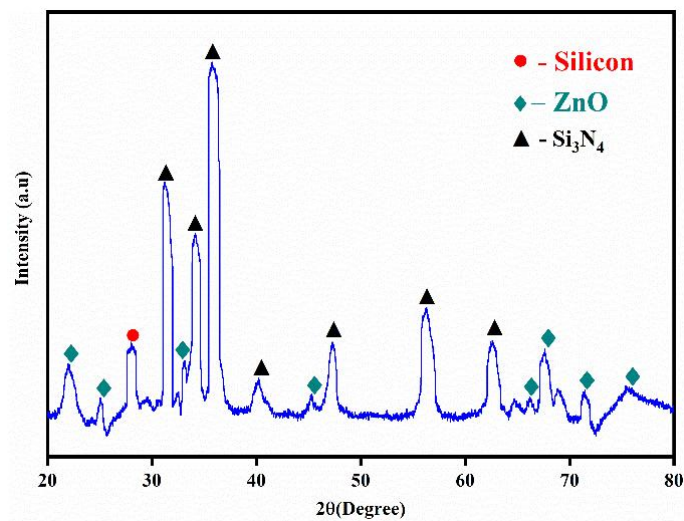


Figure 2. XRD of ZnO-Si₃N₄ mechanical blends coated solar cell.

Table 1. XRD peak positions, FWHM, and calculated crystallite size of ZnO-Si₃N₄ coated solar cell.

| 2 Theta | FWHM | Phase | Crystallite size D (nm) | Average size of Crystallite D (nm) |
|---------|------|--------------------------------|-------------------------|------------------------------------|
| 21.9 | 0.34 | ZnO | 23.80 | |
| 25.12 | 0.29 | ZnO | 28.07 | |
| 28.08 | 0.37 | Si | 22.13 | |
| 31.38 | 0.31 | Si ₃ N ₄ | 26.62 | |
| 33.19 | 0.31 | ZnO | 26.74 | |
| 34.32 | 1.11 | Si ₃ N ₄ | 7.49 | |
| 35.89 | 0.22 | Si ₃ N ₄ | 37.96 | |
| 40.29 | 0.78 | Si ₃ N ₄ | 10.85 | 27.77 |
| 45.36 | 0.41 | ZnO | 21.00 | |
| 47.36 | 0.28 | Si ₃ N ₄ | 30.98 | |
| 56.37 | 0.59 | Si ₃ N ₄ | 15.28 | |
| 62.51 | 0.87 | Si ₃ N ₄ | 10.68 | |
| 66.29 | 0.24 | ZnO | 39.53 | |
| 67.53 | 0.18 | ZnO | 53.09 | |
| 71.48 | 0.19 | ZnO | 51.51 | |
| 75.48 | 0.26 | ZnO | 38.64 | |

Depending upon the periodic arrangement of atomic particle of selected crystalline material, coherent scattering occurs which resulting in the development of sharp diffraction peaks at particular incident angles. The obtained diffraction peaks of ZnO, Si₃N₄ and ZnO-Si₃N₄ blends were matched with the standard JCPDS 36-1451 and 41-0360 to confirm the inspected material chemically [12, 13]. The XRD analysis for the ZnO-Si₃N₄ coated solar cell was indicated in Figure 2. The diffraction peaks of the ZnO-Si₃N₄ coated sample were indexed using standard JCPDS cards (ZnO: 36-1451 and Si₃N₄: 41-0360) for a more precise interpretation of the XRD results. The crystallite size of the AR coating material was determined using the Debye-Scherrer equation, with the relevant values of 2θ, FWHM, and crystallite size presented in Table 1. The findings validate the existence of crystalline ZnO and Si₃N₄ phases within the hybrid coating layer.

The surface roughness of the uncoated, ZnO, Si₃N₄ and blended ZnO-Si₃N₄ coated solar cell samples were inspected through Atomic Force Microscopy. There are three different modes of operation such as tapping mode, contact mode and non-contact mode. The most preferred method for the antireflective thin film coated solar cells was tapping mode where a cantilever setup oscillates almost equivalent to resonant frequency[14]. There are three different roughness grades: nanoscale, large scale and moderate scale. For achieving the improved light transmission with decreased light scattering, the surface roughness should be under nanoscale category [15]. The root mean square value of inspected surface roughness for bare cell, ZnO, Si₃N₄ and blended ZnO-Si₃N₄ coated solar cells were found to be 58 nm, 79 nm, 92 nm and 123 nm. The AFM studies were represented for the ZnO-Si₃N₄ coated solar in the Figure 3. The AFM research indicates that the ZnO-Si₃N₄ coated solar cell demonstrates enhanced nanoscale surface roughness relative to the uncoated cell. The increased roughness facilitates light scattering and multiple reflections of incoming photons, thus extending the optical path length within the active layer. The light-trapping effect enhances photon absorption, hence improving photocurrent generation and the PV characteristics of the AR coated solar cell.

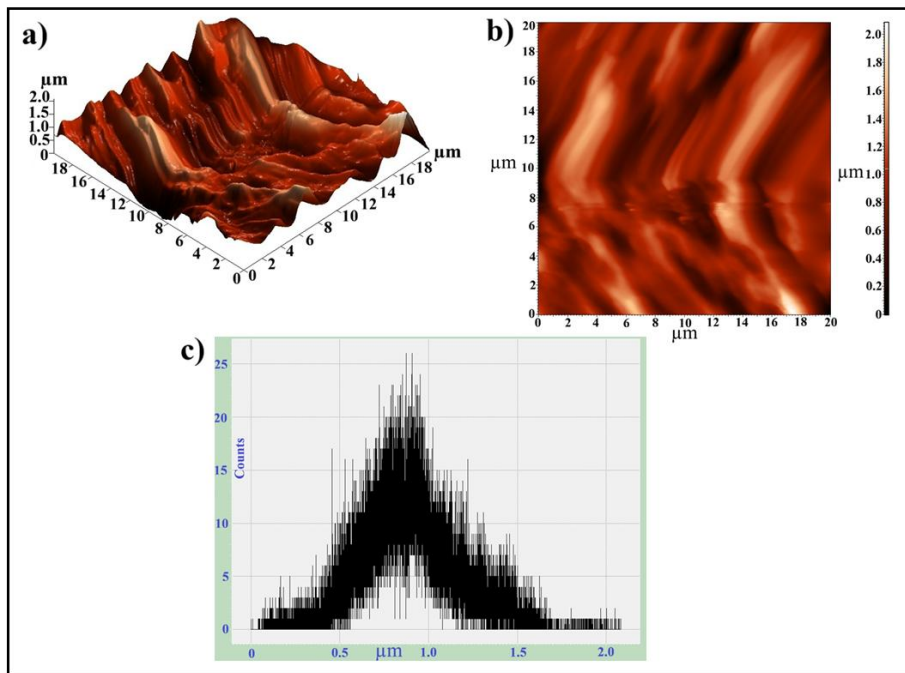


Figure 3. AFM images of the ZnO- Si₃N₄ coated substrate of the solar cell with (a) 3D surface morphology, (b) 2D surface topography, and (c) corresponding surface roughness histogram illustrating the height distribution of the coated layer.

Figure 4 displays FESEM images that depict the surface microstructure of the electrospayed AR coatings. Figure 4(a) exhibits slight non-uniformity, resulting from the droplet-based deposition mechanism of the electrospaying procedure and the partial agglomeration of nanoparticles during solvent evaporation. However, the coatings continue to produce a uniform layer throughout the solar cell surface. Moreover, the heat treatment after deposition enhanced the adhesion between the coated layer and the silicon surface, yielding stable and well-adhered antireflective coatings appropriate for solar applications. The thickness of ZnO-Si₃N₄ samples were found to be 446.6 nm (as indicated in Figure 4 (b)).

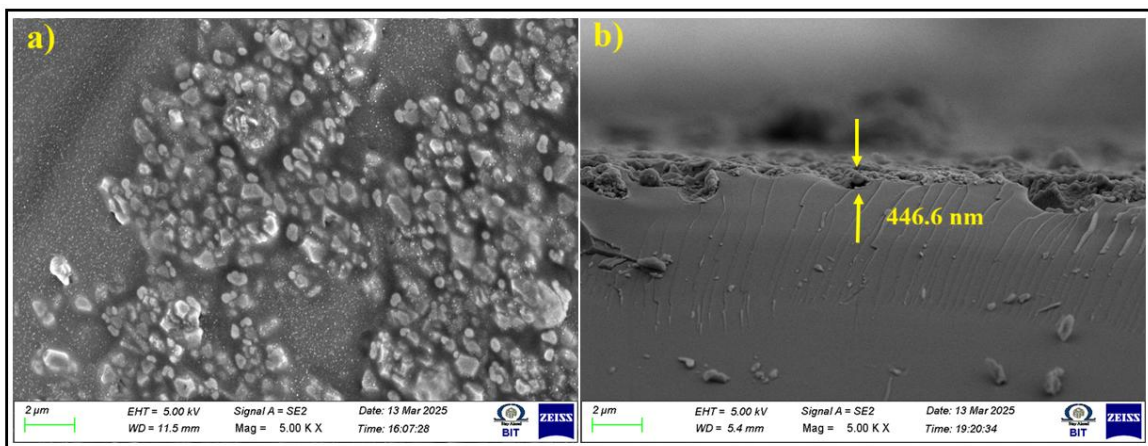


Figure 4. FESEM images of a) surface morphology and b) cross –sectional thickness of ZnO-Si₃N₄ blends coated solar cell.

The inspected solar cell samples such as bare cell, ZnO, Si₃N₄ and blended ZnO-Si₃N₄ were subjected to I-V characteristics for determining the output performance of solar cell under testing conditions under standard illumination AM 1.5G. The silver wires were soldered firmly with bus bars of coated and uncoated solar cells. With the aid of Keithley I-V source meter, the power generation capability of solar cells were been determined. The power generation will be traced as curve in the first quadrant of I-V graph. Power conversion efficiency was evaluated based on the

incurred short circuit current and open circuit voltage. The maximum possible current that can be generated by the solar cell when there is a zero voltage. Short circuit current increases with increase in intensity of incident light. Due to the antireflection coating, the short circuit current increases from 5 to 10 % than uncoated solar cell.

Open circuit voltage is the maximum voltage generated by the solar cell when there is a zero current output. It is directly rely on the generation and recombination of excitons (electron- hole pairs). The ratio of maximum power to minimum power is referred as fill factor (*FF*). The performance of bare, ZnO, Si₃N₄ and blended ZnO-Si₃N₄ coated solar cells under laboratory light source were tabulated in Table 2.

Table 2. Photocurrent-voltage measurements of ZnO, Si₃N₄ and blended ZnO-Si₃N₄ coated solar cells under laboratory light

| Specimen | <i>I</i> _{sc} (mA/cm ²) | <i>R</i> _s (Ω cm ²) | <i>R</i> _{sh} (Ω cm ²) | <i>V</i> _{oc} (V) | <i>FF</i> (%) | PCE (%) |
|--|--|--|---|----------------------------|---------------|---------|
| Bare cell | 34.22 | 0.57 | 1096 | 0.651 | 73 | 16.26 |
| ZnO | 37.85 | 0.53 | 1388 | 0.663 | 75 | 18.82 |
| Si ₃ N ₄ | 38.47 | 0.51 | 1457 | 0.673 | 77 | 19.94 |
| Blended ZnO-Si ₃ N ₄ | 39.35 | 0.46 | 1724 | 0.692 | 80 | 21.78 |

It is the measure of the maximum possible area of quadrilateral which can be traced within the generated I-V plot with respect to incident light. It also indicates the capacity of solar cell to convert light into electrical energy. Under neodymium light source, the bare solar cells, ZnO, Si₃N₄ and blended ZnO-Si₃N₄ coated solar cells were inspected and the current and voltage output were plotted in the Short-Circuit Current (*I*_{sc}) vs Open-Circuit Voltage (*V*_{oc}) graph. Due to the improved light traption by the blend coated solar cells (ZnO-Si₃N₄) than other solar cells, the power generation was observed to be higher. The observed experimental readings for ZnO-Si₃N₄ coated solar cell under controlled light source were *I*_{sc} = 39.35 mA/cm², *V*_{oc} = 0.692 V, *FF* = 80 % and PCE = 21.78 %. The I-V performance of the AR coated solar cells was further examined by evaluating the impacts of series resistance (*R*_s) and shunt resistance (*R*_{sh}). The lower *R*_s enhances charge carrier transport efficiency, whereas an elevated *R*_{sh} mitigates leakage current across the device. The higher electrical properties of the ZnO-Si₃N₄ coated solar cell result in a superior *FF* and increased power conversion efficiency relative to the uncoated cell. The photocurrent versus open circuit voltage for bare, ZnO, Si₃N₄ and blended ZnO-Si₃N₄ coated solar cells were graphically represented in Figure 5.

$$\text{Power Conversion Efficiency} = \frac{I_{sc} \times V_{oc} \times FF}{P_{in}} \quad (1)$$

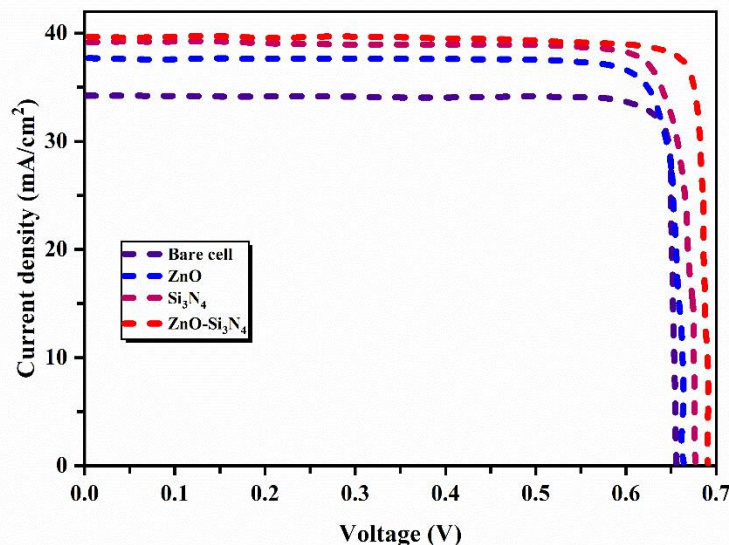


Figure 5. I-V characteristics of bare, ZnO, Si₃N₄ and blended ZnO-Si₃N₄ coated solar cells.

Electrical resistivity of coated solar cell samples ZnO, Si₃N₄ and blended ZnO-Si₃N₄ were studied through four probe method. There are four probes out of those two were supplied with current and two were measured for its voltage output [16].

Table 3. Electrical resistivity of bare, ZnO, Si₃N₄ and blended ZnO-Si₃N₄ coated cells.

| Specimen | Resistivity ($\Omega \text{ cm}$) $\times 10^{-3}$ |
|---|--|
| Bare cell | 10.53 |
| ZnO | 9.64 |
| Si ₃ N ₄ | 8.48 |
| Blended ZnO- Si ₃ N ₄ | 7.62 |

It was found that the ZnO and Si₃N₄ coated solar cells exert more electrical resistivity than ZnO-Si₃N₄ blend coated solar cell. ZnO -Si₃N₄ coated solar cell was found to exert higher carrier concentrations, more mobility of excitons and lower electrical resistivity of $7.62 \times 10^{-3} \Omega \text{ cm}$. This was mainly due to the larger grain size and smaller grain boundaries (as indicated in Table 3 & Figure 6).

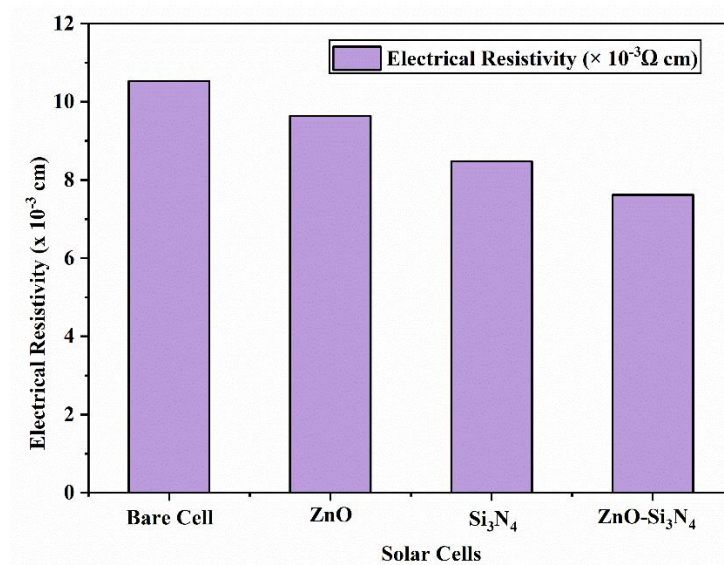


Figure 6. Electrical resistivity analysis of bare, ZnO, Si₃N₄ and blended ZnO-Si₃N₄ coated cells.

Optical studies for the bare solar cell, ZnO- Si₃N₄ coated solar cells were performed using UV Vis spectroscopy. As compared to ZnO, Si₃N₄ holds better surface layer passivation resulting in reduced reflectance. Due to the higher surface roughness, the ZnO-Si₃N₄ coated solar holds minimal light reflection and higher light transmission of 89.62 %. Increased surface roughness causes incident light gets deviated within the coated thin films [17]. This is because of the combined light trapping ability of both ZnO and Si₃N₄ as in Figure 7.

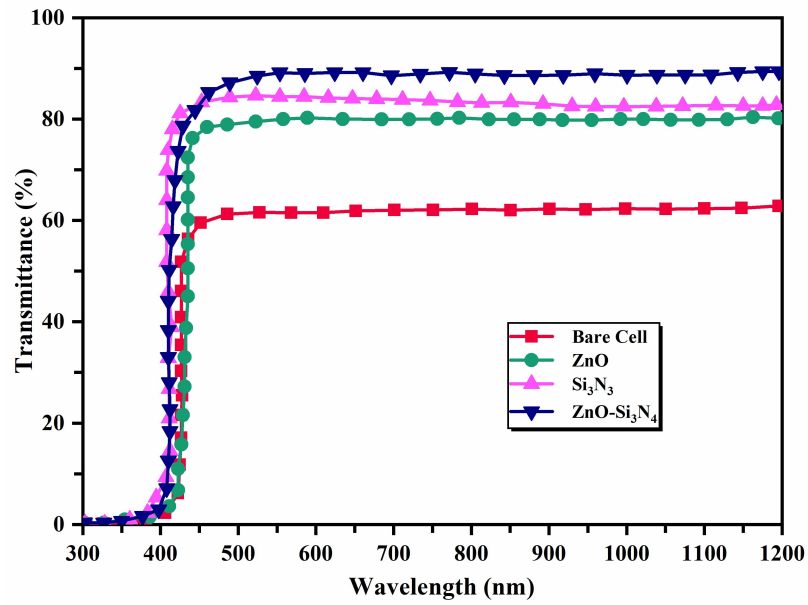


Figure 7. Optical transmittance studies of bare, ZnO, Si₃N₄ and blended ZnO-Si₃N₄ coated cells.

Reflectance spectra was evaluated through Kubelka Munk Function:

$$(\alpha \cdot hv)^{1/\gamma} = B (hv - E_g) \quad (2)$$

Where,

α : absorption coefficient

E_g: Energy of band gap

h: Planck's constant

ν : Energy of incident photon

γ : 0.5 to 2

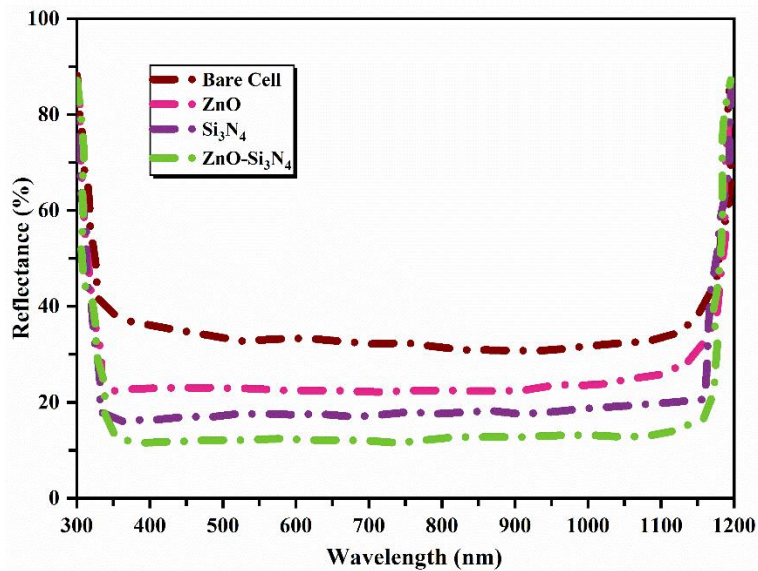


Figure 8. Optical reflectance studies of bare, ZnO, Si₃N₄ and blended ZnO-Si₃N₄ coated cells.

Because of better absorption of incident photon, the coated solar cells experiences better light transmission. The reflectance and transmittance values for various solar cells were tabulated in Table 4. However, the ZnO-Si₃N₄ blend coated solar cell delivers minimal light reflection of about 10.08 % as indicated in Figure 8 [18]. Further, the comparison study with other coated materials were reported in Table 5.

Table 4. Optical Properties in bare, ZnO, Si₃N₄ and blended ZnO-Si₃N₄ coated cells.

| Specimen | Transmittance (%) | Reflectance (%) |
|---|-------------------|-----------------|
| Bare cell | 62.46 | 35.22 |
| ZnO | 77.53 | 20.35 |
| Si ₃ N ₄ | 81.25 | 17.52 |
| Blended ZnO- Si ₃ N ₄ | 89.62 | 10.08 |

The uncoated and ARC coated solar cells (ZnO, Si₃N₄ and blended ZnO-Si₃N₄) were subjected to thermal studies using IR thermal imager. It is observed that temperatures peaked for bare solar cell and reduces for the ARC coated solar cell. The light reflection from the surface of bare cell leads to high temperature resulting in higher electrical resistivity and lower power generation output.

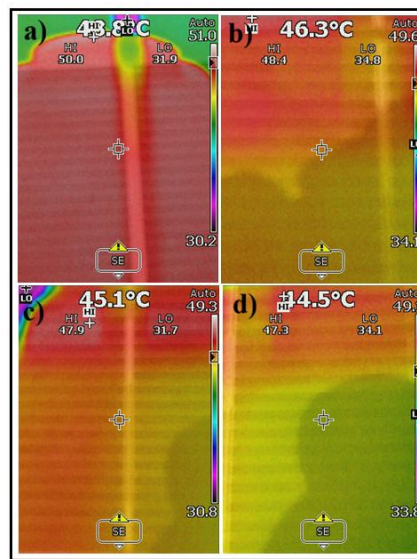


Figure 9. Thermal images of a) bare, b) ZnO, c) Si₃N₄ and d) blended ZnO-Si₃N₄ coated cells under controlled light source

The solar cells were coated ZnO-Si₃N₄ mechanical blend shows high power output, lower electrical resistivity and lower surface temperature of solar cell. Temperature of solar cell is inversely proportional to the power generation output [19]. The observed maximum and minimum solar cell temperatures for bare and ZnO-Si₃N₄ coated solar cells under laboratory light source were 48.8 °C and 44.5 °C respectively. The temperature variation for various solar cells was indicated in Figure 9. Table 5 shows the different materials that were coated in silicon substrate to improve PCE in earlier studies.

Table 5. Comparison study of transmittance and PCE of various coated materials on PV cells with the current investigation (*).

| S. No | Coating Material | Substrate (Mono/Poly) | Transmittance (%) | Improvement (%) | Reflectance (%) | Improvement (%) | PCE (%) | Improvement (%) | Reference |
|-------|------------------------------------|-----------------------|-------------------|-----------------|-----------------|-----------------|---------|-----------------|-----------|
| 1. | CeO ₂ -SiO ₂ | Polycrystalline | - | - | 11.15 | 71.52 | 20.5 | 47.48 | [20] |

| | | | | | | | | | |
|----|--|-----------------|-------|-------|-------|-------|-------|-------|------|
| 2. | WO ₃ -Al ₂ O ₃ | Monocrystalline | 92.91 | 22.84 | 7.09 | 70.9 | 23.58 | 37.41 | [21] |
| 3. | MgAl ₂ O ₄ - ZnAl ₂ O ₄ | Monocrystalline | - | - | 9 | 80.85 | 19.21 | 29.18 | [22] |
| 4. | TiO ₂ -SiO ₂ | Polycrystalline | 95.5 | 13.82 | 4 | 70.58 | 18.9 | 29.98 | [23] |
| 5. | ZnO-Si ₃ N ₄ | Polycrystalline | 89.62 | 43.48 | 10.08 | 68.61 | 21.78 | 33.94 | * |

4. Conclusions

The preferred coating technique for reducing the reflection over the incident surface of solar cells was electrospraying. This ensures the uniform coating surface than other coating techniques. The observed coating thickness through FESEM technique for bare, ZnO, Si₃N₄ and blended ZnO-Si₃N₄ coated solar cells were 219 nm, 334 nm and 446.6 nm. With the increase in surface roughness, the trapping of incident photons tends to increase for ZnO-Si₃N₄ coated solar cell of 123 nm than other solar cells. The electrical resistivity also reduces with the increased photocurrent generation. The observed electrical resistivity for bare, ZnO, Si₃N₄ and blended ZnO-Si₃N₄ coated solar cells were $10.53 \times 10^{-3} \Omega \text{ cm}$, $9.64 \times 10^{-3} \Omega \text{ cm}$, $8.48 \times 10^{-3} \Omega \text{ cm}$ and $7.62 \times 10^{-3} \Omega \text{ cm}$ respectively. The maximum and minimum power conversion efficiency was identified through I-V characterisation techniques as 16.26 % and 21.78 %. The thermal images for coated and uncoated solar cells were observed through IR thermal imager. Increased electrical resistance leads to increased solar cell temperature. The minimum solar cell temperature was experienced by ZnO-Si₃N₄ blend coated solar cell as 44.5 °C. Beyond the enhanced photovoltaic efficiency attained with the ZnO-Si₃N₄ hybrid coating, specific limitations were noted during the production process. The electrospraying process necessitates meticulous regulation of parameters like applied voltage, flow rate, and spraying distance to achieve uniform coating thickness. Also, nanoparticle aggregation during mechanical blending may influence the homogeneous distribution of the coating material. Additional optimization of the coating parameters is essential to enhance large-scale applicability and uniformity of the coating. Future endeavors will concentrate on optimizing the compositional ratio of ZnO-Si₃N₄ coatings and regulating the coating thickness to further augment light trapping and solar cell performance. The scalability of the electrospraying technology for extensive solar panels and the durability over time of hybrid AR coatings under actual environmental conditions will be examined.

Declarations

Availability of data and material: The datasets used and analyzed during the current study are available from the corresponding author on reasonable request.

Author contributions: P. Meenakshi Reddy conceived and designed the research framework; Anu Tonk and Vishal Shukla carried out the experimental and computational work; P. Vignesh and S. Karthikeyan provided critical guidance on the analytical methods and interpretation of results; Chetty Manna Sheela Rani and Raj Kumar Gupta performed the data analysis; Ramesh Kumar, P. Meenakshi Reddy and T. Thirugnanasambandhami prepared the initial draft of the manuscript. All authors have read and approved the final manuscript. All authors contributed to editorial changes in the manuscript. All authors have participated sufficiently in the work and agreed to be accountable for all aspects of the work.

Acknowledgments: Not applicable.

Funding: This research received no external funding.

Conflicts of interest: The authors declare no conflict of interest.

References

1. El-Khozondar, H.J.; El-Khozondar, R.J.; Al Afif, R.; Pfeifer, C. Modified solar cells with antireflection coatings. *International Journal of Thermofluids* 2021, 11, 100103. <https://doi.org/10.1016/j.ijft.2021.100103>
2. Gunasekaran, R.; Kaliyannan, G.V.; Refaai, M.R.A.; Gandhi, U. Sustainable manufacturing of 3D-Printed cyclic olefin copolymer coversheets with gahnite for enhanced silicon photovoltaic efficiency. *Ceramics International* 2025, 51(2), 2002-2013. <https://doi.org/10.1016/j.ceramint.2024.11.174>
3. Ji, C.; Liu, W.; Bao, Y.; Chen, X.; Yang, G.; Wei, B.; Yang, F.; Wang, X. Recent applications of antireflection coatings in solar cells. *Photonics* 2022, 9, 906. <https://doi.org/10.3390/photonics9120906>
4. Priyadarshini, B.G.; Sharma, A.K. Design of multi-layer anti-reflection coating for terrestrial solar panel glass. *Bulletin of Materials Science* 2016, 39, 683–689. <https://doi.org/10.1007/s12034-016-1195-x>
5. Law, A.M.; Jones, L.O.; Walls, J.M. The performance and durability of Anti-reflection coatings for solar module cover glass – a review. *Solar Energy* 2023, 261, 85-95. <https://doi.org/10.1016/j.solener.2023.06.009>
6. Younus, M.H.; Ali, G.G.; Salih, H.A. The reinforced optical fiber sensing with bilayer AuNPs/SiC for pressure measurement: characterization and optimization. *Journal of Physics: Conference Series* 2021, 1795, 012002. <https://doi.org/10.1088/1742-6596/1795/1/012002>
7. Sun, H.-W.; Li, L.; Gu, L.-J.; Wang, J.-S.; Zhang, L.-X.; Gu, Y.; Bao, X.-Y. Nanoimprint lithography for solar cell applications. *Journal of Nanoelectronics and Optoelectronics* 2024, 19(11), 1075–1578. <https://doi.org/10.1166/jno.2024.3534>
8. Jamaluddin, N.I.I.M.; Yusoff, M.Z.B.M.; Hussain, B.; et al. Design and simulation of different anti-reflection coatings (ARCs) to improve the efficiency of ZnO solar cells. *Journal of Optics* 2025, 54, 826–840. <https://doi.org/10.1007/s12596-024-01767-4>
9. Anu, T.; Gobikrishnan, U.; Karthikeyan, S.; Chirag, S.; Vishal, S.; Aravindan, N.; Swathi, S. Enhancing power conversion efficiency of polycrystalline silicon solar cells through ZnO/SiO₂/Al₂O₃ anti-reflective coatings via spin coating. *Journal of Ovonic Research* 2025, 21(1), 75–84. <https://doi.org/10.15251/JOR.2025.211.75>
10. Ekren, N.; Sarkin, A.S.; Sağlam, Ş. A hydrophobic antireflective and antidust coating with SiO₂ and TiO₂ nanoparticles using a new 3-D printing method for photovoltaic panels. *IEEE Journal of Photovoltaics* 2022, 12, 1014–1026. <https://doi.org/10.1109/JPHOTOV.2022.3177229>
11. Prado, R.; Beobide, G.; Marcaide, A.; Goikoetxea, J.; Aranzabe, A. Development of multifunctional sol-gel coatings: Anti-reflection coatings with enhanced self-cleaning capacity. *Solar Energy Materials and Solar Cells* 2010, 94, 1081–1088. <https://doi.org/10.1016/j.solmat.2010.02.031>
12. Iwahashi, T.; Morishima, M.; Fujibayashi, T.; Yang, R.; Lin, J.; Matsunaga, D. Silicon nitride anti-reflection coating on the glass and transparent conductive oxide interface for thin film solar cells and modules. *Journal of Applied Physics* 2015, 118(14), 145302. <https://doi.org/10.1063/1.4932639>
13. Sali, S.; Boumaour, M.; Kechouane, M.; Kermadi, S.; Aitamar, F. Nanocrystalline ZnO film deposited by ultrasonic spray on textured silicon substrate as an anti-reflection coating layer. *Physica B: Condensed Matter* 2012, 407(13), 2626-2631. <https://doi.org/10.1016/j.physb.2012.04.009>
14. Pakhuruddin, M.Z.; Yusof, Y.; Ibrahim, K.; Aziz, A.A. Fabrication and characterization of zinc oxide anti-reflective coating on flexible thin film microcrystalline silicon solar cell. *Optik* 2013, 124(22), 5397-5400. <https://doi.org/10.1016/j.ijleo.2013.03.117>
15. Hashim, A.J.; Jaafar, M.S.; Ghazai, A.J.; Ahmed, N.M. Fabrication and characterization of tetraleg zinc oxide nanostructure using evaporation methode. *Digest Journal of Nanomaterials and Biostructures* 2012, 7(2), 487–491. https://www.chalcogen.ro/487_Hashim.pdf

16. Lachiheb, M.A.; Zrir, M.A.; Nafie, N.; Abbes, O.; Yakoubi, J.; Bouaïcha, M. Investigation of the effectiveness of SiNWs used as an antireflective layer in solar cells. *Solar Energy* 2014, 110, 673–683. <https://doi.org/10.1016/j.solener.2014.10.007>
17. Shahverdi, N.; Yaghoubi, M.; Goodarzi, M.; Soleamani, A. Optimization of anti-reflection layer and back contact of Perovskite solar cell. *Solar Energy* 2019, 189, 111–119. <https://doi.org/10.1016/j.solener.2019.07.040>
18. Wang, K.X.; Yu, Z.; Liu, V.; Cui, Y.; Fan, S. Absorption enhancement in ultrathin crystalline silicon solar cells with antireflection and light-trapping nanocone gratings. *Nano Letters* 2012, 12(3), 1616–1619. <https://doi.org/10.1021/nl204550q>
19. Tavakoli, M.M.; Tsui, K.-H.; Zhang, Q.; He, J.; Yao, Y.; Li, D.; Fan, Z. Highly efficient flexible perovskite solar cells with antireflection and self-cleaning nanostructures. *ACS Nano* 2015, 9(10), 10287–10295. <https://doi.org/10.1021/acsnano.5b04284>
20. Kanmaz, I.; Tomakin, M.; Uzum, A. Analysis of CeO₂/SiO₂ double-layer thin film stack with antireflection effect for silicon solar cells. *Journal of Materials Science: Materials in Electronics* 2024, 35(22), 1497. <https://doi.org/10.1007/s10854-024-13245-5>
21. Almuflih, A.S. Electro sprayed tungsten oxide-aluminium oxide hybrid coatings: Revolutionizing anti-reflection strategies for photovoltaics. *Ceramics International* 2025, 51(12), 15581–15591. <https://doi.org/10.1016/j.ceramint.2025.01.393>
22. Mwafy, E.A.; Kaliyannan, G.V.; Darwish, A.A.A.; Motawea, M.M.; Gunasekaran, R.; Rathanasamy, R.; El-Tayeb, Z.; Elsharkawy, W.B.; Mostafa, A.M.; Palaniappan, S.K. Enhancing solar cell productivity with MgAl₂O₄-ZnAl₂O₄ blended anti-reflection coatings. *Surfaces and Interfaces* 2024, 53, 104997. <https://doi.org/10.1016/j.surfin.2024.104997>
23. Rathanasamy, R.; Velu Kaliyannan, G.; Sivaraj, S.; Saminathan, A.; Krishnan, B.; Palanichamy, D.; Uddin, M.E. Influence of Silicon Dioxide-Titanium Dioxide Antireflective Electrospayed Coatings on Multicrystalline Silicon Cells. *Advances in Materials Science and Engineering* 2022, 2022, 9444524. <https://doi.org/10.1155/2022/9444524>



© 2026 by the authors. Submitted for possible open access publication under the terms and conditions of the Creative Commons Attribution (CC BY) license (<http://creativecommons.org/licenses/by/4.0/>).